International Journal of Biological Macromolecules 187 (2021) 789–799

Contents lists available at ScienceDirect

International Journal of Biological Macromolecules

journal homepage: www.elsevier.com/locate/ijbiomac

Correlation between rheological measurements and morphological features of lignocellulosic micro/nanofibers from different softwood sources

Ferran Serra-Parareda [a], Quim Tarrés [a,b], Pere Mutjé [a,b], Ana Balea [c], Cristina Campano [c], Jose Luis Sánchez-Salvador [c], Carlos Negro [c], Marc Delgado-Aguilar [a,*]

[a] LEPAMAP-PRODIS Research group, University of Girona, C/ Maria Aurèlia Capmany, 61 – 17003 Girona, Spain
[b] Chair on Sustainable Industrial Processes, University of Girona, Maria Aurèlia Capmany, 6, 17003 Girona, Spain
[c] Department of Chemical Engineering and Materials, University Complutense of Madrid, Avda Complutense s/n, 28040 Madrid, Spain

ARTICLE INFO

Keywords:
Lignocellulosic micro/nanofibers
Rheological behavior
Morphology

ABSTRACT

The transition of nanocellulose production from laboratory to industrial scale requires robust monitoring systems that keeps a quality control along the production chain. The present work aims at providing a deeper insight on the main factors affecting the rheological behavior of (ligno)cellulose micro/nanofibers (LCMNFs) and cellulose micro/nanofibers (CMNFs) and how they could correlate with their characteristics. To this end, 20 types of LCMNFs and CMNFs were produced combining mechanical refining and high-pressure homogenization from different raw materials. Aspect ratio and bending capacity of the fibrils played a key role on increasing the viscosity of the suspensions by instigating the formation of entangled structures. Surface charge, reflected by the cationic demand, played opposing effects on the viscosity by reducing the fibrils' contact due to repulsive forces. The suspensions also showed increasing shear-thinning behavior with fibrillation degree, which was attributed to increased surface charge and higher water retention capacity, enabling the fibrils to slide past each other more easily when subjected to flow conditions. The present work elucidates the existing relationships between LCMNF/CMNF properties and their rheological behavior, considering fibrillation intensity and the initial raw material characteristics, in view of the potential of rheological measurements as an industrial scalable characterization technology.

1. Introduction

Nanocellulose (NC) is an outstanding and renewable nanomaterial that has recently attracted significant attention in many research areas, mainly due to its interesting properties and characteristics, which have been subject of multiple studies for a wide range of applications [1–4]. NC can be found in different forms, depending on the production method and the resulting properties, including crystallinity, morphology, or chemical composition. Indeed, several studies have referred to cellulose nanofibers (CNFs), lignocellulosic nanofibers (LCNFs), cellulose nanocrystals (CNCs) or even microfibrillated cellulose (MFC) under the designation of NC [5,6]. All these kinds of NCs can be produced from a wide variety of raw materials, including softwood, hardwood, agricultural residues, recovered paper or any other lignocellulosic biomass, although the origin may have some influence on the resulting characteristics of the nanostructured material. The production process of LCNFs and CNFs usually encompasses two different stages to deconstruct the hierarchical structure of lignocellulosic fibers. On the one hand, the use of chemical or enzymatic pretreatments is often recommended to reduce the energy consumption during the second stage, consisting of an intensive mechanical treatment, to increase the ratio of nanosized fibers in the resulting suspension and to provide some surface functional groups that might be of interest [7–9]. On the other, the mechanical treatment, also known as fibrillation stage, may be conducted by means of several equipment, including but not limited to high-pressure homogenization, grinding, or microfluidization, exhibiting some differences in terms of performance [10,11].

One of the main attributes of CNFs and LCNFs is their ability to form entangled network-like structures, leading to highly viscous suspensions even at low consistency, mainly due to their high aspect ratio and hydrophilicity [12]. Such viscous behavior has considerably drawn the attention of researchers, as it could provide useful information on their processability, storage and transportation, but also due to its potential in several applications [13–15]. In addition, rheology has also been

* Corresponding author.
E-mail address: m.delgado@udg.edu (M. Delgado-Aguilar).

https://doi.org/10.1016/j.ijbiomac.2021.07.195
Received 25 June 2021; Received in revised form 27 July 2021; Accepted 30 July 2021
Available online 2 August 2021

reported as a useful characterization tool to understand the morphology and fibril interaction mechanisms of CNFs and LCNFs [16].

Despite the great potential for CNFs and LCNFs in multiple and diverse sectors, their upscaling for production and commercialization is not still developed, mainly due to the limitations imposed by chemical pretreatments in terms of high manufacturing costs, challenging recovery of reagents, excessive depolymerization of fiber components, presence of highly reactive functional groups, and the lack of an efficient drying and redispersing system able to preserve the initial properties of CNFs and LCNFs [17–21]. Besides, albeit enzymatic pretreatments have been reported to offer a more environmental friendly and cheaper approach, their upscaling is also limited, as they require long residence times in heated bioreactors and, indeed, the use of chemicals is not fully avoided [22,23].

The challenges posed by chemical and enzymatic pretreatments glimpse the possibility of an entire mechanical production line, adopting mechanical refining as pretreatment. Mechanical refining is an industrially available technology which has been traditionally used in the pulp and paper sector to improve paper properties, though, it is also attractive as fiber pretreatment prior to mechanical fibrillation of the pulps [1,24]. Mechanical refining is based on the application of shearing forces that enhance fiber swelling, while breaking down the fiber structure leading to shorter and highly fibrillated fibers, which has been reported to contribute to the fibrillation stage during LCNF and CNF production. [25,26]. At laboratory scale, some examples of mechanical refining include PFI mills and Valley piles, which are based in different principles but are representative of large-scale plate and cone refiners. As extensively reported, the effects produced by the Valley pile on the fibers could potentially contribute to the production of a more homogeneously fibrillated product than other pretreatments [24]. The combination of both refining and homogenization processes is expected to produce CNF and LCNF suspensions with a significant amount of microscopic fibers, usually over 50%, exhibiting external fibrillation in the nano domain, as well as individualized nanofibers. Owing to such characteristics, the resulting material can be referred to as cellulose micro/nanofibers (CMNFs) or (ligno)cellulose micro/nanofibers (LCMNFs) [27,28]. Thereby, disposing of enzymatic and chemical pretreatments may contribute to cost-efficient production of CNFs and LCNFs, indeed, there seems to be an increasing trend towards CMNFs and LCMNFs rather than other NC grades, especially for large volume applications.

Apart from the abovementioned challenges, other important factor limiting the large-scale production of NC is the lack of high-speed and accurate measurement tools and methods that could serve as monitoring parameters during production processes, as authors have pointed out in a recent review [29]. To the date, the most accepted characterization methods so far are based on multiparameter processes to obtain a complete roster of properties, or even a single quality indicator. Such is the case of Desmaisons et al. [30], where a multi-criteria method was proposed, enabling the obtention of a single quantitative grade with the purpose of monitoring the production of CNFs and LCNFs. However, such multiparameter approaches are usually limited to laboratory use and not scalable, as they are excessively time consuming. Another possibility would be the characterization of CNFs from a unique parameter. The use of microscopy methods has been already proposed, mainly electron and atomic force microscopy (AFM), to determine the ratio of nanosized fibers and their dimensions [31]. Nonetheless, obtaining representative and reliable results is also time consuming and expensive, as excessive images are required and data acquisition is a tedious task. Although data acquisition could be optimized by means of artificial vision techniques, images should be systematically taken regardless the sample characteristics, which may lead to overlooking of relevant structures [32–34]. In a simpler way, Gu et al. [35] proposed the water retention value (WRV) as a reliable parameter to monitor the fibrillation process. However, besides being a time-consuming technique, in a recent work, the application of the WRV as a monitoring parameter was found to not correlate with the fibrillation degree of LCNFs and LCMNFs. This was attributed to the fact that WRV, which is highly associated to the specific surface area, is also influenced by the chemical composition of the fibrils which may unpredictably change due to lignin release during mechanical processes [28]. In the same work, authors proposed cationic demand (CD) to monitor fibrillation, but this measurement is severely influenced by conductivity and pH [36].

Therefore, there is a real need of orientating research towards appropriate monitoring methods enabling industrial scalability, while providing relevant and valuable information about the production process. To overcome this situation, some researchers have focused their efforts on the rheological behavior of NC suspensions, which is well known to be influenced by both structural and individual fibril characteristics [16,37,38]. In addition, rheology offers the possibility of inline measurement along the production chain, which would contribute to eliminate the lag created between process and characterization. Inline viscometers have already been successfully implemented at industrial scale in other sectors, but its use in the NC production sector is not still developed as for the uncertainty regarding the relationships between rheology and the rest of the properties [29]. Thereby, the present work stands as a thoughtful and innovative study on the relationships between rheology and properties of mechanically obtained CMNFs and LCMNFs, providing useful information for future mass production of such nanostructured material [39].

The widespread morphologies, as well as different surface chemistries, usually drive to varied properties and, presumably, to different rheological behavior. Such properties largely depend on the initial pulp and the intensity of the mechanical treatment. Accordingly, and for the sake of comparison, the present work considers the production of LCMNFs and CMNFs from two different softwood sources, namely (i) spruce (*Picea abies*) and (ii) pine (*Pinus radiata*). Precisely, pine pulps had undergone thermomechanical, kraft and bleached kraft treatments, whereas the spruce pulp was a thermomechanical pulp. The selection of such raw materials is based on evaluating the rheological behavior of the suspensions by varying the initial fiber source and fiber treatment. Besides, different mechanical intensities were imparted to the pulps by setting a constant refining intensity and then passing the suspensions through a high-pressure homogenizer by progressively increasing the number of passes from 3 to 9 and pressure from 300 to 900 bar.

2. Experimental

2.1. Materials

Bleached thermomechanical pulp from spruce (BTMP) was kindly provided by Norske Skog Saugbrugs (Halden, Norway), thermomechanical pulp from pine (TMP) was kindly supplied by Zubialde, S. A. (Aizarnazabal, Spain), unbleached kraft pulp from pine (UKSP) and bleached kraft pulp from pine (BKSP) were kindly provided by Celulosa Arauco y Constitución (Chile). These pulps were used to produce the LCMNFs and CMNFs. All reagents used in the present work were acquired at Sigma-Aldrich and were used as received with no further purification.

2.2. Methods

2.2.1. Raw material and pretreated pulps characterization

The chemical composition of the raw and refined pulps was determined as according to NREL and TAPPI standards. The extractive content was evaluated via acetone Soxhlet extraction according to TAPPI standard T204. Total lignin, hemicellulose and cellulose contents were assessed according to NREL/TP-510-42,618 standard from the extractive-free pulps. Briefly, 300 mg of extractive-free fibers were hydrolyzed with 3 mL of 72 wt% H_2SO_4 at 30 °C. After one hour hydrolysis, 84 g of deionized water were added and the mixture was introduced in an autoclave for one hour at 121 °C, to be later vacuum filtered. Klason

Table 1
HPH sequences.

HPH identification	Number of passes through the HPH at each operating pressure		
	300 bar	600 bar	900 bar
3	3	0	0
3_1	3	1	0
3_3	3	3	0
3_3_1	3	3	1
3_3_3	3	3	3

lignin remained on the top of the filter, while the soluble lignin fraction was obtained through UV–Visible spectrophotometry of the filtrate. Hemicellulose and cellulose were determined by means of HPLC. In parallel, the ash content was quantified by combustion at 525 °C, according to TAPPI standard T211.

The crystallinity of the samples, in terms of crystallinity index (CrI) was measured by means of X-ray diffraction (XRD) using a Bruker D8 Advance diffractometer with a Cu-Kα radiation and operating at 45 kV and 40 mA. The 2 Theta (2θ) angular region from 4° to 33° was scanned with steps of 0.05° and a step time of 40 s. The CrI was calculated using the method reported by Segal et al., (1959) [40], which is based on the ratio of the intensity of the 002 peak (I_{002}, $2\theta = 22.6$), and the intensity of minimum between 18 and 19° (I_{am}) (Eq. (1)).

$$CrI. = \frac{I_{002} - I_{am}}{I_{002}} \cdot 100 \quad (1)$$

The morphology of the pulps, including parameters such as mean fiber length and diameter, was evaluated by means of a MorFi Compact Analyzer from TechPap (Grenoble, France) which analyses about 30,000 fibers per test aided by the software MorFi v9.2. Additionally, the pulps were observed by means of a Zeiss Axio Lab.A1 optical microscope fitted with an optical microscope camera Zeiss AxioCam ERc 5 s (Carl Zeiss Microscopy GmbH, Göttingen, Germany) at x5 magnification.

2.2.2. LCMNFs and CMNFs production

Pulps were disintegrated in a laboratory scale pulper according to ISO 5263-1 standard. Briefly, 30 g (over dry weight) were introduced in the pulper and water was added until achieving a pulp consistency of 1.5 wt%, to be later disintegrated for 20 min at 3000 rpm. The resulting pulp suspension was vacuum-filtered using a 400-mesh screen and adjusted to 10 wt% consistency. This process was repeated four times until obtaining 120 g of each pulp. The disintegrated pulps were subjected to mechanical refining in a Valley pile using a 500 g (wet weight) and setting a residence time of 60 min. The resulting materials from this stage were four different pulps refined at same intensity in a Valley pile.

The refined pulps were passed through a high-pressure homogenizer (HPH) NS1001L PANDA 2 K-GEA (GEA Niro Soavy, Parma, Italy) at 1 wt % consistency and by progressively increasing the number of passes and pressure. Samples were taken at different stages of the homogenization process, obtaining the sequences reported in Table 1. Accordingly, each refined pulp led to 5 types of LCMNFs with different fibrillation degree, attaining a total of 20 types of LCMNFs with either different fiber source, pulping treatment, and HPH sequence.

2.2.3. Characterization of LCMNFs and CMNFs

The obtained LCMNFs and CMNFs were characterized in terms of yield of nanofibrillation, transmittance at 600 nm, cationic demand (CD), water retention value (WRV) and aspect ratio. The yield of nanofibrillation was determined by centrifuging 0.1 g (on dry weight basis) at 0.2 wt% consistency at speed of 4500 rpm for 20 min (150 mm radius; 3402 G-force). The sediment, which contains the non-fibrillated fraction, was separated and oven-dried at 105 °C until constant weight. The yield of nanofibrillation is the ratio between the nanosized fibers (calculated by the difference between the initial dry mass and the dried sediment) and the initial dry mass. Transmittance values were recorded at 600 nm wavelength using a UV–Vis spectrophotometer Shimadzu UV-160A, setting the consistency at 0.1 wt% and using distilled water as reference. CD was determined by means of back potentiometric titration using a Mütek PCD 04 particle charge detector (BTG Instruments, Germany). For its determination, 0.1 g (dry weight) were mixed with a known amount of excess of cationic polymer polyDADMAC (0.001 N). The mixture was then centrifugated for 90 min at speed of 4000 rpm (70 mm radius; 1254 G-force). Then, 10 mL from the supernatant were taken to the Mütek and tritiated with anionic polymer PesNa (0.001 N) until 0 mV were reached. From the volume of PesNa needed to neutralize the excess of cationic polymer and the total amount of initial polyDADMAC, the CD can be calculated as detailed in previous works [41]. The WRV was measured by separating the non-bonded water out of the LCMNFs suspensions and then calculating the amount of bonded water per gram of dry sample. Such determination was carried out by centrifuging the suspensions for 30 min at 2400 rpm in polypropylene bottles equipped with a nitrocellulose membrane at the bottom. Further details of the characterization procedures can be found in the literature [42,43].

The morphology of the LCMNFs and CMNFs was evaluated via the determination of the aspect ratio and the observation through transmission electron microscopy (TEM). Aspect ratio was determined by a simplified gel point methodology based on the sedimentation of LCMNFs and CMNFs according to [44]. Besides, the LCMNFs suspensions were observed at the National Centre of Electronic Microscopy (Madrid, Spain) by JEOL JEM 1400 microscope (JEOL, Tokio, Japan) operating at 100 kV of accelerating voltage and following the methodology developed by Campano et al., (2020) [45]. Briefly, 15 μL of a 10% solution of Poly-L-Lysine were deposited on a 200 mesh formvar/copper grid in order to convert its surface into cationic and hydrophilic. Then, 12 μL of 0.005 wt% LCMNFs or CMNFs were placed on the treated grids and left to dry before TEM observation.

The rheological behavior of the suspensions was evaluated by means of a Couette-type (co-axial cylinder) PCE-RVI 2 V1L rotational viscosimeter (PCE Instruments, Germany). The apparent viscosities (η) of the suspensions at 1 wt% consistency were recorded by increasing the rotational speed from 0.5 to 200 rpm. The shear rate (γ) et each rotational speed was calculated from the dimensions of the spindle and the

Table 2
Chemical composition and CrI of the initial and pretreated pulps.

Pulp	Cellulose	Hemicellulose	Lignin[a]	Extractives	Ashes	CrI
	(wt%)	(wt%)	(wt%)	(wt%)	(wt%)	(%)
BTMP	48.9 ± 0.4	20.5 ± 0.2	29.3 ± 0.4	0.8 ± 0.1	0.5 ± 0.1	75.3
BTMP_mec	46.2 ± 0.4	22.9 ± 0.2	29.4 ± 0.4	0.9 ± 0.1	0.5 ± 0.1	76.1
TMP	48.5 ± 0.5	18.3 ± 0.3	30.5 ± 0.6	0.6 ± 0.2	2.1 ± 0.1	71.5
TMP_mec	47.9 ± 0.5	22.9 ± 0.2	27.0 ± 0.3	0.7 ± 0.1	1.4 ± 0.1	73.3
UKSP	73.8 ± 0.4	16.0 ± 0.2	9.2 ± 0.2	< 0.3	0.8 ± 0.1	82.5
UKSP_mec	74.2 ± 0.4	16.6 ± 0.2	8.2 ± 0.2	< 0.3	0.8 ± 0.1	81.1
BKSP	86.2 ± 0.5	8.2 ± 0.2	4.0 ± 0.3	0.7 ± 0.1	1 ± 0.1	87.9
BKSP_mec	85.3 ± 0.5	8.7 ± 0.2	3.9 ± 0.3	1.2 ± 0.1	0.9 ± 0.1	87.0

[a] Total lignin content determined as the sum of the acid-insoluble and acid-soluble lignin.

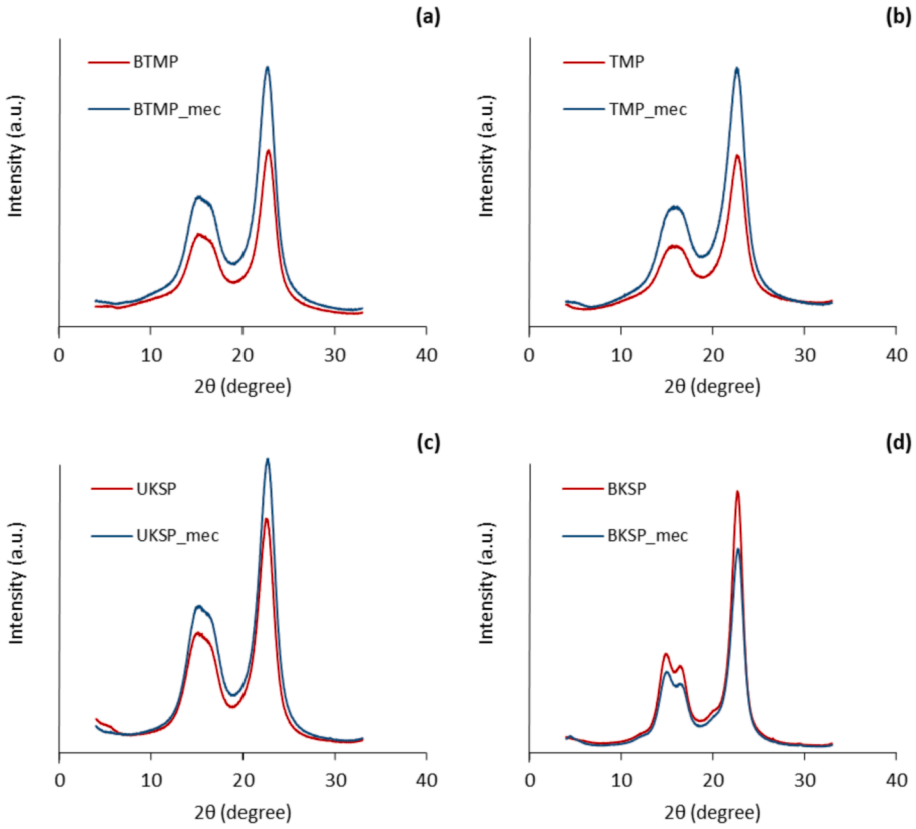

Fig. 1. X-ray diffraction patterns of (a) BTMP and BTMP_mec, (b) TMP and TMP_mec, (c) UKSP and UKSP_mec, (d) BKSP and BKSP_mec.

vessel, following Eq. (2), finally obtaining a shear rate range from 0.25 to 165.83 s^{-1}.

$$\gamma = 2 \cdot \frac{2\pi N_i}{60} \cdot \frac{R_0^2}{R_0^2 - R_i^2} \tag{2}$$

where N_i is the rotational speed in rpm, and R_0 and R_i are the radius of the vessel and spindle with values of 1.10 and 0.95 mm, respectively. The logarithmic plots of the flow curves were fitted to the Oswald-de Waele equation (Eq. (3)) [13,18,46].

$$\eta = k \cdot \gamma^{-n} \tag{3}$$

where k and n are identified as the consistency and flow indexes, respectively. Briefly, the consistency index is typically used as an overall measure of the suspension's viscosity, whereas the flow index evaluates the non-Newtonian degree of the suspension. In this context, flow index of zero indicates a Newtonian fluid, whereas n values below 1 reveal pseudoplastic behavior (shear-thinning).

3. Results and discussion

3.1. Raw and pretreated pulps characterization

The chemical composition of the starting pulps (BTMP, TMP, UKSP and BKSP) and the mechanically pretreated pulps (BTMP_mec, TMP_mec, UKSP_mec and BKSP_mec) is provided in Table 2. In addition, the X-ray diffraction patterns of the pulps are presented in Fig. 1, from which the crystallinity index (CrI) is calculated and included in Table 2.

As expected, thermomechanical pulps (BTMP and TMP) presented lower cellulose contents, below 50 wt% in both cases, than kraft pulps, with values up to 73.8 and 86.2 wt% for UKSP and BKSP, respectively. Instead, the lignin content was higher in thermomechanical pulps, around the 27–30 wt%, whereas the kraft treatments visibly reduced the lignin content to 9.2% and 4.0 wt% for the unbleached and bleached pulp, respectively. The effect of the kraft treatment on the hemicellulose content was not as harsh as with lignin, though, the bleaching of the kraft pulps was shown to be more effective on reducing the hemicellulose content. The higher contents of cellulose in kraft pulps, being cellulose the most crystalline compound within the fiber cell wall, also led to greater CrI in these pulps, obtaining values near to 75% in the case of thermomechanical pulps, both BTMP and TMP. It was also found that the contents of extractives and ashes in the selected pulps was not excessive, which from a technical viewpoint is interesting as keeping low amounts of these components has been reported to enhance the nanofibrillation yield during the fibrillation process [47].

It is worth mentioning that the bleaching step imparted to the BTMP had a slight, almost negligible, effect on the chemical constituents of the pulp, as it was noticed that the composition of Norwegian spruce wood, which is the initial fiber source, is not significantly different from BTMP [48]. In fact, bleaching of thermomechanical pulps usually aim at removing chromophores to increase pulp brightness, hence, preserving the chemical structure of the fiber, instead of removing residual lignin and hemicellulose as in the case of chemical pulps bleaching. From this point of view, it is concluded that the derived results from TMP and BTMP can be directly compared neglecting the effect of bleaching step in the case of BTMP.

After submitting the pulps to mechanical refining, the most noticeable effect was found to be a slight lignin content reduction (around 3 wt %) in TMP, also contributing to an increase of the cellulose ratio and CrI of this sample. The effect of mechanical refining on the BTMP was not as pronounced as in the case of TMP, even being possible to consider the small variations as insignificant. The lignin reduction in TMP due to refining can be attributed to mechanical peeling and delamination of the fiber cell wall, which by consequence promotes lignin release [49]. In a different but comparable scenario, the shearing forces in the high-pressure homogenizer (HPH) have also been reported to promote

Table 3
Morphological parameters of the initial and pretreated pulps.

Pulp	Mean fiber length[a]	Mean fiber diameter	Fines content[b]	Aspect ratio
	(μm)	(μm)	(%)	(−)
BTMP	1178 ± 42	29.8 ± 0.2	52 ± 3	39.5
BTMP_mec	821 ± 34	28.9 ± 0.8	62 ± 2	28.4
TMP	808 ± 66	31.1 ± 0.7	30 ± 1	26.0
TMP_mec	377 ± 26	29.3 ± 1.1	55 ± 2	12.9
UKSP	837 ± 62	26.1 ± 0.4	34 ± 4	32.1
UKSP_mec	430 ± 35	20.7 ± 0.5	46 ± 1	20.8
BKSP	1691 ± 48	24.7 ± 0.7	12 ± 2	68.5
BKSP_mec	449 ± 40	21.8 ± 1.1	33 ± 0	20.6

[a] Mean fiber length weighted in length.
[b] Fines are considered as particles which length is below 75 μm.

lignin release in thermomechanical pulps [28]. Apart from the lignin content, the mechanical pretreatment may also promote the disordering of the crystalline regions in kraft pulps, resulting in a reduction of the CrI, as observed in both UKSP and BKSP samples. Similar effects on the crystallinity and composition of fibers as consequence of mechanical refining have been previously reported [50,51].

Besides chemical composition, mechanical refining also affects the morphology of the pulps mainly by imparting fiber cutting and generating fine particles. Such morphological changes are reported in Table 3 where the main morphological parameters are shown. Optical images of the samples are also provided in Fig. 2 to deepen into the morphology of the pulps.

It becomes apparent that refining made the fibers much shorter by reducing the mean fiber length and releasing fibrils, hereby referred to as fines. Many of such fines are found at the fibers' surface of refined pulps in the form of external fibrillation, as observed in Fig. 2, fact that contrasts with the smoother appearance of unrefined pulps. In addition, mechanical refining had a significant impact on fiber length, being of a lower magnitude in the case of diameter. This explains the decrease of the aspect ratio after refining. Although such effects resulting from pulp refining (i.e. fiber cutting and fines generation) have been typically regarded as undesired effects in the papermaking sector, they could potentially promote pulp fibrillation in the HPH and avoid clogging of the pressure chambers, which is interesting from a technical viewpoint [24].

Table 3 also shows that the mean fiber length, as well as mean fiber diameter, decreased more severely in pine pulps (TMP, UKSP and BKSP) than in the spruce pulp (BTMP), from which it is concluded that refining had a stronger influence, in morphological terms, on pine pulps. Further, the effect of refining on the chemical composition became more evident in the case of TMP than in BTMP.

3.2. Characterization of the CMNFs and LCMNFs suspensions

The resulting LCMNFs and CMNFs suspensions were characterized in terms of yield of nanofibrillation, CD, transmittance at 600 nm of wavelength ($T_{600\ nm}$) and WRV. These parameters have been previously used by several authors and, albeit their indirect nature, they have been reported to provide a good indication of the LCMNFs and CMNFs characteristics.

As expected, the yield of nanofibrillation increased with the number of passes and pressure in the HPH regardless of the type of pulp. The fibrillated BTMP reached yields around the 20% at the most intense HPH sequence, contrarily to TMP, which exhibited yields below 10%. Regarding kraft pulps, UKSP presented a yield close to 18% at 3 + 3 + 3 HPH sequence, whereas BKSP showed a slightly lower content of nanofibers (15.5%) at the same HPH stage. The obtention of lower yields in BKSP with respect to UKSP is mainly ascribed to the presence of residual lignin in the latter pulp that inhibits the formation of fibril bundles and prevents the re-agglomeration of the nanofibrillated parts. On the contrary, bleaching of kraft pulps has been found to eliminate most of the remaining residual lignin (see Table 2) and, thus, incentive fibrils aggregation by increasing the number of hydroxyl groups at the fiber surface [52,53]. The fact that TMP provided lower yields than UKSP and BKSP is explained by the excessive amount of lignin in this sample that binds the fibrils together and hinder its release from the original bundle during the fibrillation process. Interestingly, BTMP offered significantly higher yields than TMP and somewhat higher than those of UKSP and BKSP. Such differences between TMP and BTMP in terms of nanofibrillation yield could be attributed to the inherent influence of fiber source, to the notably higher content of fines in BTMP_mec, and to the somewhat lower content of extractives and ashes in the spruce pulp. In this context, albeit the role of extractives and ashes during pulp fibrillation is yet to be consolidated, it is accepted that the presence of low amounts of non-structural elements (i.e., extractives and ashes) could positively influence the separation of nanofibers from the original bundle [47,54].

The relatively low yields obtained in comparison to other CNF grades produced by chemical or enzymatic pretreatments, where yields can reach up to 95% and 40%, respectively, explain the low transmittance of the suspensions [55]. Optical transmittance can be used as an indirect indicator of the yield of nanofibrillation, since light scattering during transmittance tests is highly dependent on the fibril's shape and dimensions. Hence, the presence of micro-sized fibers with thicker diameters than nanofibers would justify the low transmittance values of the suspensions. It is noted that even though BTMP owned higher yields

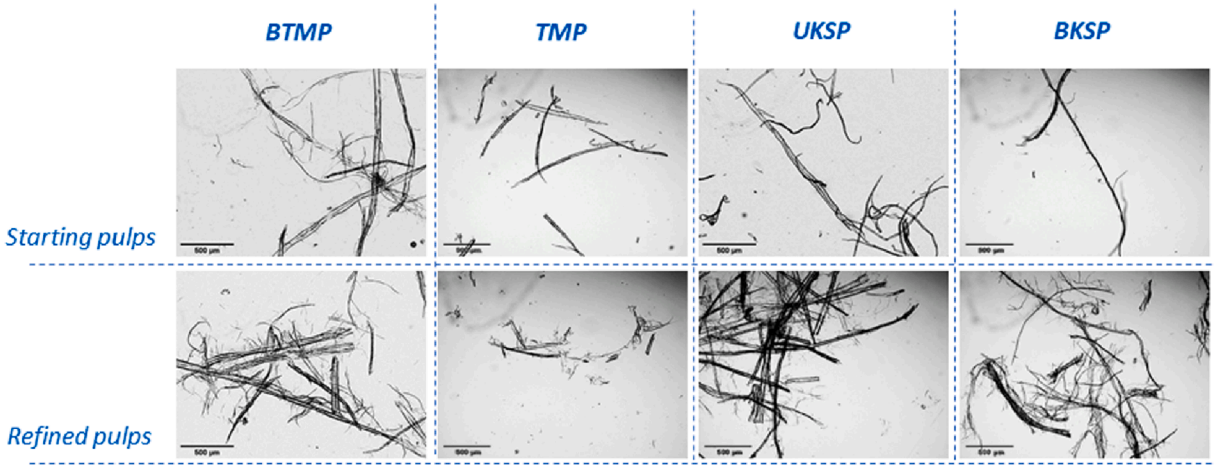

Fig. 2. Optical microscopy images of initial pulps (BTMP, TMP, UKSP and BKSP) and their respective refined pulps.

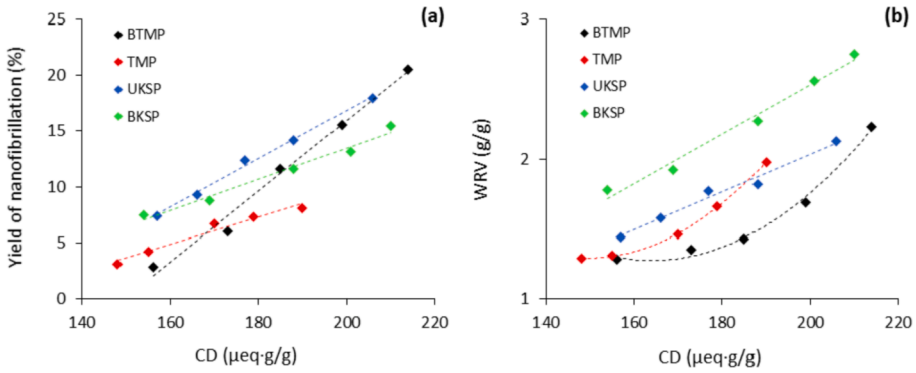

Fig. 3. Evolution of the yield of nanofibrillation (a) and WRV (b) with the CD.

than UKSP and BKSP, which in principle should derive into higher transmittance values, the presence of lignin interfering the analyses provides BTMP lower transmittances. Overall, it is concluded from the low yields and low transmittance values that the obtained suspensions were a mix of both micro and nanosized fibers, the main reason why the authors have considered reasonable to label the suspensions as micro/nano fibers (LCMNFs and CMNFs, depending on the presence of lignin).

CD was found to increase in an overall range of 150 to 215 μeq/g, mainly depending on the HPH intensity, being less affected by the type of pulp. This was partially expected, as the initial pulps had not been chemically modified by the introduction of charged groups (i.e., TEMPO-mediated oxidation) that could influence the surface charge of the pulps. Likewise, similar CD values in micro/nanofibers from different feedstocks produced by similar approach have been previously reported [56,57].

The CD has proved to correlate well with the specific surface area and nanofibrillation yield, making the parameter a suitable candidate, albeit not ideal, to monitor the mechanical production of micro/nanofibers [28]. Indeed, in this work the CD is observed to evolve linearly with the nanofibrillation yield within the different homogenization sequences, as shown in Fig. 3.a. Some limitations of the CD as a monitoring parameter include the great variability of surface charge depending on the pretreatment conditions and raw material, and the fact that CD would require sophisticated correlations to be inline monitored in a large-scale production process. Hence, in this study the CD is not viewed as a potential monitoring parameter, but as an indicator of the surface charge to study the relationships between surface charge and rheology [13].

The submission of the pretreated pulps to successive fibrillation steps also contributed to increasing the WRV of the micro/nanofibers. BKSP owned the higher WRV reaching up to 2.75 g/g at the highest HPH intensity, which is understandable owing to the larger content of cellulose and thus, higher water retention capacity. Beyond chemical composition, WRV also depends on the available surface area, which is increased with the HPH intensity. Such combined effect between chemical composition and fibrillation degree explains the fact that even though BTMP contained a higher content of nanofibers and presumably larger surface availability than UKSP, both pulps yielded similar WRV owing to

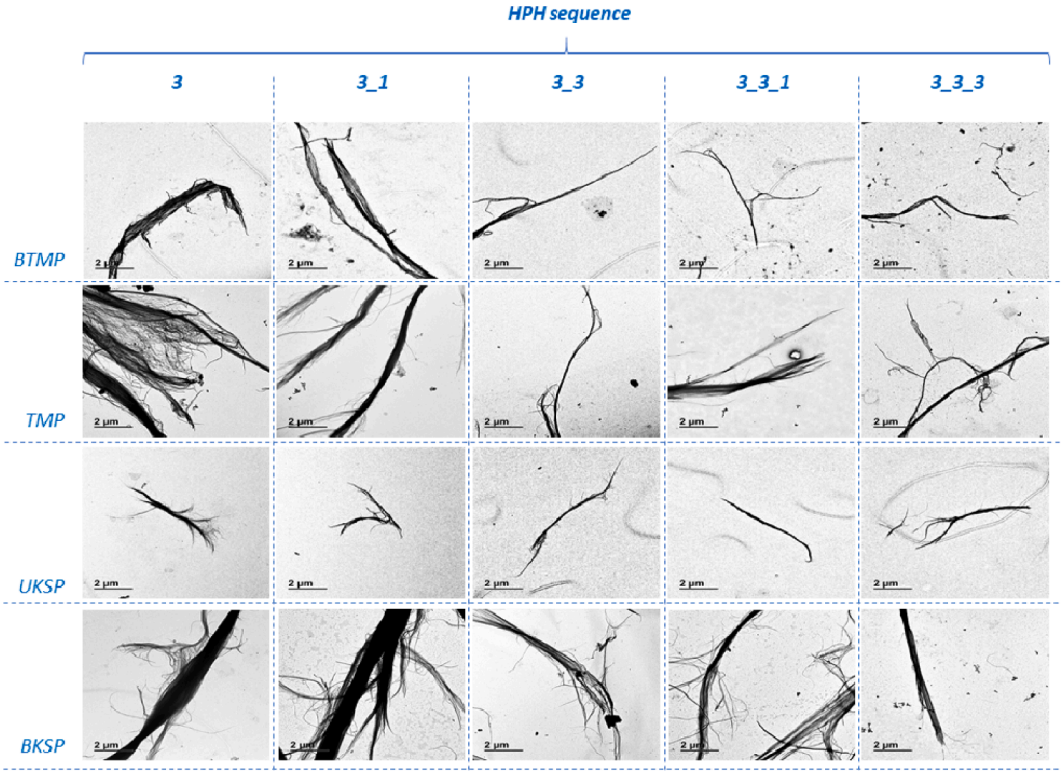

Fig. 4. TEM images of the LCMNFs from BTMP, TMP, UKSP and BKSP at different HPH stages.

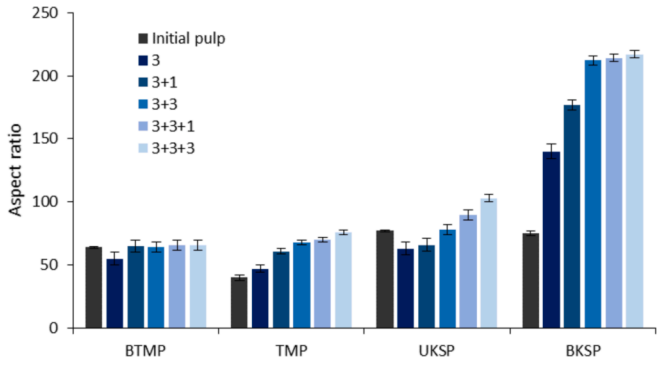

Fig. 5. Evolution of the aspect ratio with the homogenization intensity.

the larger content of cellulose in UKSP. Besides, the micro/nanofibers from TMP, with high lignin content and low nanofibrillated fraction, presented the lowest WRV.

As long as the chemical composition of the pulp does not vary during the fibrillation treatment, as for kraft pulps, the WRV linearly correlates with the specific surface area (SSA) and hence can be used as monitoring parameter of the fibrillation degree [35,58]. Though, in thermomechanical pulps, some lignin may be detached from the fibrils structure as consequence of the shearing forces in the HPH. As the lignin content is reduced due to homogenization, the hydrophilicity of the sample becomes higher and thus the WRV increases [28]. In such cases, the WRV may increase not only because of the higher fibrillation degree, but also due to unpredictable variations on the chemical composition of the sample, finally making the WRV a non-adequate parameter to monitor the production of high-lignin content nanofibers. Fig. 3.b shows the evolution of the WRV with the CD as the homogenization intensity is increased. It is observed that the WRV of the micro/nanofibers from BKSP and UKSP increased linearly with the CD. Such tendency was not repeated in thermomechanical pulps, since the WRV tended to increase gradually above the expected linearity resulting into a second-order polynomial tendency. In the case of the chemically obtained pulps (kraft, both UKSP and BKSP), most of the lignin was removed by means of its solubilization. However, those thermomechanically obtained pulps still exhibited some easier to remove lignin by means of shear forces, which may contribute to the higher enhancement of the WRV as HPH intensity increases.

3.3. Morphology of the micro/nanofibers

Surface charge and morphology are probably the most influencing factors governing the rheological behavior of micro-nanofibrillated suspensions [59,60]. In this work, the morphology of the fibrillated samples was assessed through TEM observation (Fig. 4), whereas the mean aspect ratio of the micro/nanofibers was quantified as a relevant morphological parameter through the gel-point methodology (Fig. 5).

TEM images in Fig. 4 evidence the presence of widespread morphologies with branched structures and external fibrillation, which is a typical morphological trait of those NC grades obtained by fully mechanical processes. Also, some fibril bundles are observed at the initial HPH stages, whereas the homogenization treatment is seen to enhance the presence of slender particles. Indeed, Fig. 5 shows that the mean aspect ratio of the fibrils increased with the HPH intensity principally in pine pulps (TMP, UKSP and BKSP), being such increments less significant for the spruce pulp (BTMP). Precisely, BKSP fibrils experienced a pronounced increase of the aspect ratio from 75 to 217, whereas those homogenized lignin-containing pulps (UKSP, TMP and BTMP) provided lower increments in the range of 40 to 103.

From TEM images it is also possible to see that BKSP fibrils are apparently thicker and longer than UKSP ones. As stated during the characterization of the LCMNFs, the residual lignin in UKSP could be

Table 4
Characterization of the micro-nanofibers.

Pulp	HPH sequence	Yield (%)	CD (μeq/g)	$T_{600\ nm}$ (%)	WRV (g/g)
BTMP_mec	3	2.9 ± 0.3	156 ± 2	4.1 ± 0.1	1.28 ± 0.12
	3_1	6.0 ± 0.4	173 ± 3	4.7 ± 0.2	1.35 ± 0.09
	3_3	11.6 ± 0.4	185 ± 1	7.0 ± 0.1	1.43 ± 0.10
	3_3_1	15.6 ± 0.3	199 ± 2	9.7 ± 0.0	1.69 ± 0.05
	3_3_3	20.6 ± 0.6	214 ± 2	11.9 ± 0.1	2.23 ± 0.05
TMP_mec	3	3.1 ± 0.6	148 ± 4	2.5 ± 0.1	1.29 ± 0.08
	3_1	4.2 ± 0.9	155 ± 5	3.1 ± 0.2	1.31 ± 0.13
	3_3	6.7 ± 0.4	170 ± 3	5.9 ± 0.1	1.46 ± 0.03
	3_3_1	7.3 ± 0.4	179 ± 4	7.0 ± 0.1	1.66 ± 0.06
	3_3_3	8.1 ± 0.3	190 ± 2	7.4 ± 0.2	1.98 ± 0.11
UKSP_mec	3	7.4 ± 0.1	157 ± 2	4.2 ± 0.3	1.44 ± 0.06
	3_1	9.3 ± 0.5	166 ± 2	6.5 ± 0.1	1.58 ± 0.02
	3_3	12.4 ± 0.6	177 ± 4	7.4 ± 0.1	1.77 ± 0.03
	3_3_1	14.2 ± 0.7	188 ± 5	9.9 ± 0.1	1.82 ± 0.09
	3_3_3	17.9 ± 0.6	206 ± 4	12.5 ± 0.0	2.13 ± 0.08
BKSP_mec	3	7.5 ± 0.8	154 ± 2	5.4 ± 0.1	1.78 ± 0.10
	3_1	8.8 ± 0.6	169 ± 3	6.8 ± 0.2	1.92 ± 0.11
	3_3	11.6 ± 0.5	188 ± 4	7.2 ± 0.1	2.27 ± 0.04
	3_3_1	13.1 ± 0.3	201 ± 2	9.5 ± 0.1	2.56 ± 0.07
	3_3_3	15.5 ± 0.7	210 ± 2	12.7 ± 0.1	2.75 ± 0.03

interfering between the cellulosic fibrils making them easier to separate from the original bundle under shear forces, finally yielding higher nanofibrillation yields (see Table 4) and lower diameters. Such residual lignin may also promote fibrils rupture perpendicularly to their axis, critically reducing the fibrils' length and thus, their aspect ratio [53,61]. Besides, higher cellulose contents, as for BKSP, may contribute to strong inter-fibrillar bondings and mitigate the cutting effect imparted by the homogenization process, obtaining longer particles and higher aspect ratios [62]. In the case of thermomechanical pulps, as for TMP and BTMP, the elevated lignin contents of the fibrils, which are also probably more rigid than the kraft fibrils, may promote fibrils' rupture indistinctively at different zones, thus, contributing to widespread morphologies and lower aspect ratios.

3.4. Rheological behavior

The rheological behavior of LCMNFs was evaluated by means of a Couette-type rheometer by progressively increasing the shear rate. Fig. 6 shows the logarithmic plots of the apparent viscosity (η) as a function of the shear rate (γ) of the obtained suspensions, prepared from different raw materials at subsequent HPH sequences.

From Fig. 6 it is observed that the apparent viscosity increased with the homogenization intensity regardless of the shear rate measurement. The viscous behavior of LCMNFs in water suspensions can be principally, albeit not completely, attributed to the tendency of the fibrils to form entangled structures. This leads to more hindering interactions between the fibrils and decrease in their mobility, finally providing higher viscosity measurements [13]. The entanglement ability of LCMNFs can be principally ascribed to morphological features. For instance, fibrils with elevated aspect ratios will be more likely to interlace and create entangled networks. It must be noted that other fibrillation treatments (i.e., ultra-fine grinder, ball milling) may impart different and varied effects, in morphological terms, on the fibrils and consequently different rheological behaviors may be expected [63,64]. The importance of morphology on the suspensions' viscosity is also observed in those highly nanofibrillated NC grades such as CNF and CNC [38]. Indeed, it is already possible to find some models able to predict important morphological features of CNC and CNF out of rheological measurements [65].

Within morphological features, aspect ratio has been typically seen as a predominant parameter governing the rheological behavior of LCMNFs suspensions. However, as observed in Fig. 6, both UKSP and BKSP provided similar viscosity measurements, while being the aspect

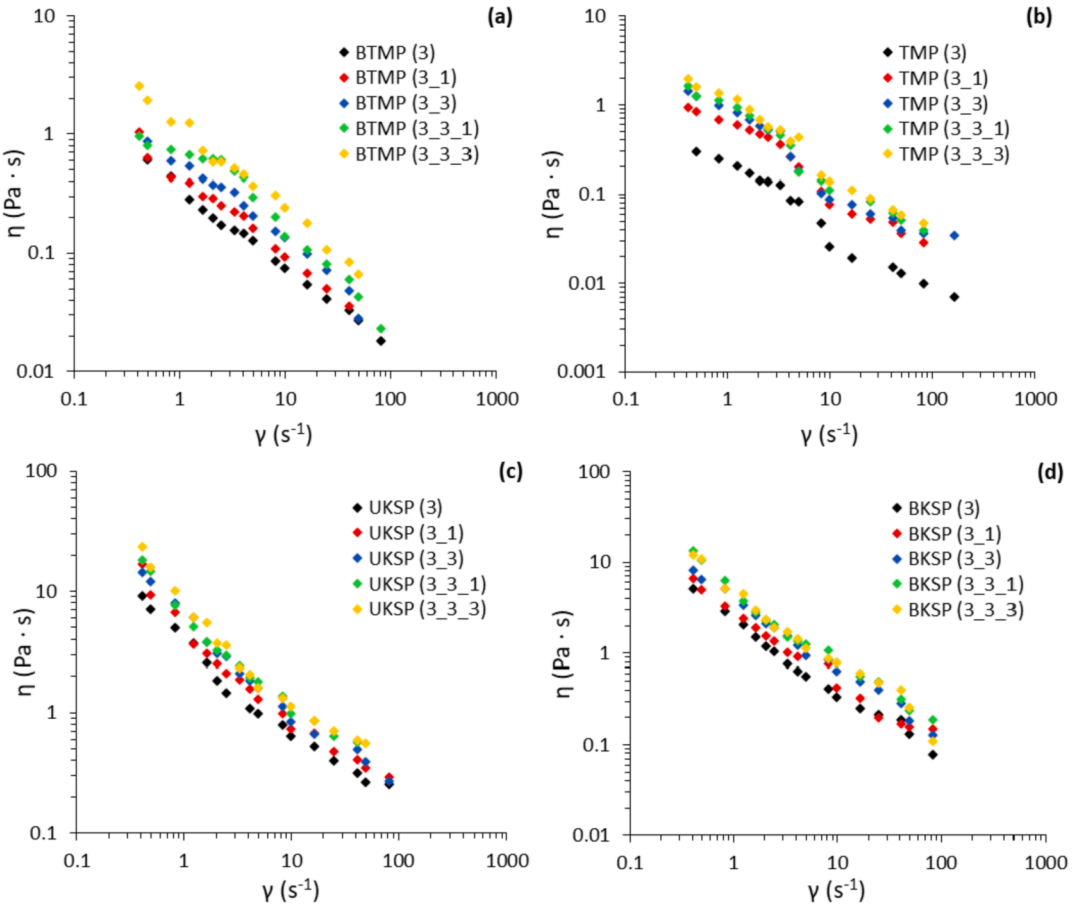

Fig. 6. Evolution of apparent viscosity (η) with shear rate (γ) of the LCMNFs from (a) BTMP, (b) TMP, (c) UKSP and (d) BKSP at different HPH intensities.

ratio of BKSP appreciably higher than UKSP. Likewise, the greater viscosity observed in UKSP with respect to thermomechanical pulps (TMP and BTMP) was not consistent with the small discrepancies observed between the aspect ratio of the samples. Furthermore, the literature reports similar, or even lower, aspect ratios for CNFs than the ones obtained in this work, though, exhibiting much higher viscosities [43,44]. For instance, the aspect ratio measured by the gel-point methodology of a highly fibrillated CNF product obtained via TEMPO-mediated oxidation followed by high-pressure homogenization was reported to be in the range of 90–100 [66].

Overall, the viscosity of the suspensions is suggested to be influenced by other variables besides aspect ratio. In this context, the entanglement capacity of the fibrils may be also pushed by the presence of more flexible fibrils which are more likely to bend and interlace one-another. Such flexibility has been found to decrease with increasing fibrils thickness [67]. Then, UKSP fibrils are expected to be more flexible than BKSP ones, fact that could aid their entanglement. Besides, the significantly different chemical compositions between kraft and thermomechanical pulps may also affect the bending capacity of the fibrils. Precisely, the presence of elevated lignin contents in TMP and BTMP may provide firmness and inflexibility to the fibrils, making them behave more as rigid rather than deformable particles [68]. In addition, the thermomechanical pulping processes to obtain TMP and BTMP may also damage the fiber cell wall in comparison to kraft process, and this could also limit their bending capacity. High lignin contents could also reduce the water-bonding capacity of the fibrils, contributing to increase the amount of free water and reducing the viscosity of the suspension. In general, the chemical composition of thermomechanical pulps, with high lignin contents, is hypothesized to be the main responsible for the obtention of low aspect ratios, more rigid fibrils with limited bending capacity, and poor water-retaining capacities, all together contributing to lower viscosities in comparison to BKSP and UKSP suspensions.

Surface charge, hereby reflected in the CD parameter, has also been reported to play an important role for the interaction between fibrils surfaces. It is accepted that increasing the surface charge due to fibrillation (Table 4) would induce electrostatic repulsion forces between the fibrils. Such repulsion forces between surfaces should reduce the entanglement capacity of the fibrils, finally deriving into lower viscosity measurements [13,69]. However, it is also possible to hypothesize that increasing the surface charge may contribute to the capacity of the fibrils to bond water owing to the larger amount of anionic groups at the fibrils' surface. In this case, the amount of free water in the suspension will decrease, providing higher viscosity to the suspensions. The role of surface charge on the viscosity measurements will be posteriorly elucidated by means of a quantitative evaluation of the rheological curves. Overall, it is possible to state that the overall viscosity of the suspension may result from a combination of different, maybe opposing, effects that change with the fibrillation degree.

Fig. 6 also evidence a clear overall tendency of the viscosity to decrease as the shear rate increases, suggesting shear thinning behavior of the suspensions. Such shear-thinning behavior exhibited by LCMNFs has been broadly described in the literature and attributed to the disruption of the fibril networks and aggregates when subjecting the suspension to flow, finally allowing the orientation of the fibrils in the flow direction and hence reducing the apparent viscosity of the suspensions [70,71]. Such disentanglement ability shown by the fibrils may be understood by the existing interactions between surfaces, which at the same time depend on the surface charge (CD) and swelling capacity (WRV) of the fibrils. In this sense, increasing the repulsion forces between fibrils (higher CD) could lead to an easier break down of the

Table 5
Rheological parameters of the micro/nanofibers suspensions at various fibrillation cycles estimated using the power law model.

Pulp	HPH sequence	k ($Pa \cdot s^n$)	n (−)	R^2 (−)
BTMP	3	0.349	0.338	0.995
	3_1	0.456	0.324	0.987
	3_3	0.616	0.307	0.979
	3_3_1	0.781	0.299	0.944
	3_3_3	1.201	0.278	0.989
TMP	3	0.222	0.281	0.969
	3_1	0.520	0.272	0.965
	3_3	0.789	0.270	0.948
	3_3_1	0.889	0.257	0.970
	3_3_3	1.107	0.239	0.979
UKSP	3	3.706	0.309	0.971
	3_1	4.987	0.280	0.964
	3_3	6.042	0.257	0.980
	3_3_1	6.642	0.244	0.949
	3_3_3	7.679	0.233	0.961
BKSP	3	2.178	0.253	0.985
	3_1	2.824	0.256	0.984
	3_3	3.873	0.247	0.993
	3_3_1	4.816	0.234	0.981
	3_3_3	4.830	0.219	0.976

entangled networks by slipping one-another more easily, ultimately contributing to fibrils' orientation under flow conditions and so, to shear-thinning behavior [72]. Besides, the presence of more swollen fibrils with more bounded water on the surface (higher WRV) should reduce the frictional forces between fibrils, enabling them to slide past each other more easily under flow [73]. As a result, it is suggested that both CD and WRV play an important role on the shear-thinning behavior. For TMP and BTMP fibrils, the shear-thinning behavior may also decrease by the presence of rougher surfaces due to the presence of lignin and the damage suffered during thermomechanical pulping treatments.

Towards a quantitative assessment between characterization and rheological variables, the data obtained from the flow curves (Fig. 6) was fitted to a power law model to obtain the consistency index (k) and the flow behavior index (n). Typically, k values can be used as an overall indicator of the suspension's viscosity, whereas n values could be related to the shear-thinning behavior of the suspension. Accordingly, highly viscous suspensions would yield greater k values, whereas the n values would decrease as the suspensions becomes more shear-thinning. The values of k, n and correlation factors (R^2) are reported in Table 5 for the different types of LCMNFs. Fig. 7.a presents the evolution of k with the aspect ratio of the LCMNFs calculated from the gel-point methodology. Further, the CD is plotted against k in Fig. 7.b to elucidate the role of surface charge on the viscosity of the suspensions.

Table 5 reports relatively high, close to 1, correlation factors (R^2), suggesting the validity of the power law model to predict the rheological parameters k and n. Parameter k (Fig. 7.a) is observed to increase with the aspect ratio for all LCMNFs types, confirming the above-mentioned relationship between viscosity and aspect ratio. The observed k values for UKSP are somewhat higher than the ones of BKSP, while being the aspect ratio of BKSP notably higher. As mentioned before, fibrils' entanglement could be aided by the presence of more flexible fibrils as in the case of UKSP, which therefore would contribute to the suspension's viscosity. Further, surface charge could also be influencing such results. The role of surface charge can be elucidated from Fig. 7. For instance, BKSP (3 + 3) and UKSP (3) provided similar k values, while being the aspect ratio and CD of BKSP (3 + 3) significantly higher than UKSP (3). Considering that the aspect ratio enhances the suspension's viscosity, it is assumed that the CD plays an opposing effect on such viscosity by inducing repulsive forces between fibrils and contributing to their disentanglement. Such assumption may not be inferred to highly nanofibrillated NC grades, where the great surface charge may drastically reduce the amount of free water and increase the suspension's viscosity. Besides, interestingly, it was found that both BTMP and TMP, with similar aspect ratios and chemical compositions, returned k values in the same range.

Regarding to the shear thinning behavior, the gradual decrease of the flow index n with the homogenization intensity indicates increasing shear-thinning behavior through the HPH stages. As explained before, this can be due to higher CD and WRV that enable the easiest disentanglement of the fibril networks when subjecting the suspension to flow. As an example, BKSP provided relatively higher WRVs than UKSP, and so it was more shear-thinning (lower n values). In addition, kraft fibrils, with smoother surfaces, showed higher shear-thinning behavior than BTMP and TMP suspensions at same HPH stage.

4. Conclusions

Monitoring the mechanical production of (ligno)cellulose micro/nanofibers (LCMNFs) at large scale requires a fast, rather inline, characterization system that provides useful information on the fibrils morphology and suspensions. Rheological measurements could successfully fulfil this need, though a deeper understanding on the mechanism governing the rheological behavior of such suspensions is required. In this work, a complete set of 20 types of LCMNFs were prepared combining mechanical refining and high-pressure homogenization. Each LCMNFs type differed from the other either in fiber source, fiber pulping treatment, or fibrillation degree. Mainly depending on these variables, the obtained LCMNFs displayed nanofibrillation yields in the range of 3–21 wt%, cationic demands around 150–210 μeq/g,

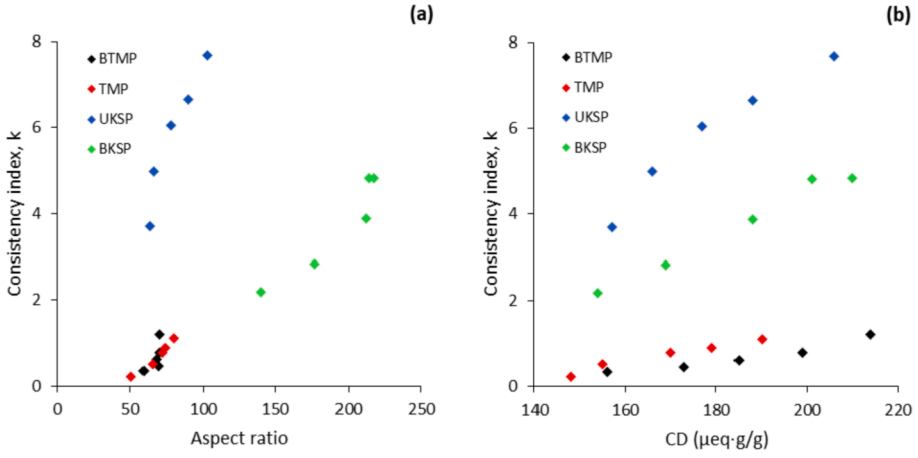

Fig. 7. Evolution of the consistency index k, with the aspect ratio (a) and cationic demand (b).

water retention values between 1 and 3 g/g and aspect ratios in the range of 50–230. Relationships between characterization and rheological parameters were evaluated both via qualitative and quantitative ways. Results showed that the entanglement capacity of the fibrils, mainly dominated by surface fibrillation and rigidity of the fibrils, imparted a predominant effect on the suspensions' viscosity. Further, increasing surface charge due to fibrillation was found decrease the viscosity of the suspensions by reducing the number of contact points. Surface charge and water retention capacity of the fibrils played a more crucial role on defining the shear thinning behavior of the suspensions, by allowing an easiest disruption of the fibril networks when subjected to flow. The relationships established between characterization and rheological parameters are viewed as an interesting starting point to ease the scale-up, at least in terms of characterization methods, of such nanostructured lignocellulosic materials.

CRediT authorship contribution statement

Ferran Serra-Parareda: Investigation, Writing – original draft. **Quim Tarrés:** Data curation, Validation, Methodology. **Pere Mutjé:** Project administration, Funding acquisition. **Ana Balea:** Investigation, Writing – original draft. **Cristina Campano:** Investigation, Data curation. **Jose Luis Sánchez-Salvador:** Investigation. **Carlos Negro:** Conceptualization, Funding acquisition, Project administration, Supervision. **Marc Delgado-Aguilar:** Conceptualization, Writing – review & editing, Project administration, Supervision.

Acknowledgements

Authors wish to acknowledge the financial support of the Spanish Economy and Competitiveness Ministry to the Project NANOPROSOST (references CTQ2017-85654-C2-1-R and CTQ2017-85654-C2-2-R), as well as the support of Universidad Complutense de Madrid and Banco de Santander for the grant of J.L. Sanchez-Salvador (CT17/17). Also thanks to the Spanish Ministry of Science and Innovation for the Juan de la Cierva aid of Cristina Campano (Ref. FJC2019-040298-I) and the Spanish National Centre of Electronic Microscopy for the support during image acquisition. Marc Delgado-Aguilar is a Serra Húnter Fellow.

References

[1] T. Lindström, C. Aulin, A. Naderi, M. Ankerfors, Microfibrillated cellulose, in: Encycl. Polym. Sci. Technol, John Wiley & Sons, Inc., Hoboken, NJ, USA, 2014, pp. 1–34, https://doi.org/10.1002/0471440264.pst614.
[2] A. Isogai, Emerging nanocellulose technologies: recent developments, Adv. Mater. (2020) 2000630, https://doi.org/10.1002/adma.202000630.
[3] R. Arvidsson, D. Nguyen, M. Svanström, Life cycle assessment of cellulose nanofibrils production by mechanical treatment and two different pretreatment processes, Environ. Sci. Technol. (2015), https://doi.org/10.1021/acs.est.5b00888.
[4] J.H. Kim, B.S. Shim, H.S. Kim, Y.J. Lee, S.K. Min, D. Jang, et al., Review of nanocellulose for sustainable future materials, Int. J. Precis. Eng. Manuf. 2 (2015) 197–213, https://doi.org/10.1007/s40684-015-0024-9.
[5] J. Wang, X. Liu, T. Jin, H. He, L. Liu, Preparation of nanocellulose and its potential in reinforced composites: a review, J. Biomater. Sci. Polym. Ed. 30 (2019) 919–946, https://doi.org/10.1080/09205063.2019.1612726.
[6] Y. Habibi, L.A. Lucia, O.J. Rojas, Cellulose nanocrystals: chemistry, self-assembly, and applications, Chem. Rev. 110 (2010) 3479–3500.
[7] T. Saito, S. Kimura, Y. Nishiyama, A. Isogai, Cellulose nanofibers prepared by TEMPO-mediated oxidation of native cellulose, Biomacromolecules 8 (2007) 2485–2491, https://doi.org/10.1021/bm0703970.
[8] M. Henriksson, G. Henriksson, L.A. Berglund, T. Lindström, An environmentally friendly method for enzyme-assisted preparation of microfibrillated cellulose (MFC) nanofibers, Eur. Polym. J. 43 (2007) 3434–3441, https://doi.org/10.1016/j.eurpolymj.2007.05.038.
[9] A. Moral, R. Aguado, A. Tijero, Cationization of native and alkalized cellulose: mechanismand kinetics, Cellul. Chem. Technol. 50 (2016) 109–115.
[10] Q. Tarrés, H. Oliver-Ortega, S. Boufi, M. Àngels Pèlach, M. Delgado-Aguilar, P. Mutjé, Evaluation of the fibrillation method on lignocellulosic nanofibers production from eucalyptus sawdust: a comparative study between high-pressure homogenization and grinding, Int. J. Biol. Macromol. 145 (2020) 1199–1207, https://doi.org/10.1016/j.ijbiomac.2019.10.046.
[11] K.L. Spence, R.A. Venditti, O.J. Rojas, Y. Habibi, J.J. Pawlak, A comparative study of energy consumption and physical properties of microfibrillated cellulose produced by different processing methods, Cellulose 18 (2011) 1097–1111, https://doi.org/10.1007/s10570-011-9533-z.
[12] P. Tingaut, T. Zimmermann, G. Sèbe, Cellulose nanocrystals and microfibrillated cellulose as building blocks for the design of hierarchical functional materials, J. Mater. Chem. 22 (2012) 20105–20111.
[13] M.A. Hubbe, P. Tayeb, M. Joyce, P. Tyagi, M. Kehoe, K. Dimic-Misic, et al., Rheology of nanocellulose-rich aqueous suspensions: a review, Bioresources 12 (2017) 9556–9661.
[14] O. Nechyporchuk, M.N. Belgacem, J. Bras, Production of cellulose nanofibrils: a review of recent advances, Ind. Crop. Prod. 93 (2016) 2–25, https://doi.org/10.1016/j.indcrop.2016.02.016.
[15] C. Liu, H. Du, L. Dong, X. Wang, Y. Zhang, G. Yu, et al., Properties of nanocelluloses and their application as rheology modifier in paper coating, Ind. Eng. Chem. Res. 56 (2017) 8264–8273.
[16] H. Kangas, P. Lahtinen, A. Sneck, A.M. Saariaho, O. Laitinen, E. Hellén, Characterization of fibrillated celluloses. A short review and evaluation of characteristics with a combination of methods, Nord. Pulp Pap. Res. J. 29 (2014) 129–143.
[17] M.V.G. Zimmermann, C. Borsoi, A. Lavoratti, M. Zanini, A.M. Jattera, R.M. C. Santana, Drying techniques applied to cellulose nanofibers, J. Reinf. Plast. Compos. 35 (2016) 628–643.
[18] E. Lasseuguette, D. Roux, Y. Nishiyama, Rheological properties of microfibrillar suspension of TEMPO-oxidized pulp, Cellulose 15 (2008) 425–433, https://doi.org/10.1007/s10570-007-9184-2.
[19] L. Kuutti, H. Pajari, S. Rovio, J. Kokkonen, M. Nuopponen, Chemical recovery in TEMPO oxidation, Bioresources 11 (2016) 6050–6061.
[20] M. Delgado-Aguilar, I. González, Q. Tarres, M. Alcalà, M.A. Pelach, P. Mutje, Approaching a low-cost production of cellulose nanofibers for papermaking applications, Bioresources 10 (2015) 5345–5355.
[21] A. Serra, I. González, H. Oliver-Ortega, Q. Tarrès, M. Delgado-Aguilar, P. Mutjé, Reducing the amount of catalyst in TEMPO-oxidized cellulose nanofibers: effect on properties and cost, Polymers (Basel) 9 (2017), https://doi.org/10.3390/polym9110557.
[22] S. Janardhnan, M. Sain, Bio-treatment of natural fibers in isolation of cellulose nanofibres: impact of pre-refining of fibers on bio-treatment efficiency and nanofiber yield, J. Polym. Environ. 19 (2011) 615–621, https://doi.org/10.1007/s10924-011-0312-6.
[23] S. Kalia, K. Thakur, A. Celli, M.A. Kiechel, C.L. Schauer, Surface modification of plant fibers using environment friendly methods for their application in polymer composites, textile industry and antimicrobial activities: a review, J. Environ. Chem. Eng. 1 (2013) 97–112, https://doi.org/10.1016/j.jece.2013.04.009.
[24] A.F. Turbak, F.W. Snyder, K.R. Sandberg, Microfibrillated cellulose, a new cellulose product: properties, uses, and commercial potential, J. Appl. Polym. Sci. 37 (1983).
[25] B.W. Jones, R. Venditti, S. Park, H. Jameel, B. Koo, Enhancement in enzymatic hydrolysis by mechanical refining for pretreated hardwood lignocellulosics, Bioresour. Technol. 147 (2013) 353–360, https://doi.org/10.1016/j.biortech.2013.08.030.
[26] M. Jonoobi, A.P. Mathew, K. Oksman, Producing low-cost cellulose nanofiber from sludge as new source of raw materials, Ind. Crop. Prod. 40 (2012) 232–238, https://doi.org/10.1016/j.indcrop.2012.03.018.
[27] C.A. de Assis, M.C. Iglesias, M. Bilodeau, D. Johnson, R. Phillips, M.S. Peresin, et al., Cellulose micro- and nanofibrils (CMNF) manufacturing - financial and risk assessment, Biofuels Bioprod. Biorefin. (2018), https://doi.org/10.1002/bbb.1835.
[28] F. Serra-Parareda, Q. Tarrés, M.À. Pèlach, P. Mutjé, A. Balea, M.C. Monte, et al., Monitoring fibrillation in the mechanical production of lignocellulosic micro/nano fi bers from bleached spruce thermomechanical pulp, Int. J. Biol. Macromol. 178 (2021) 354–362, https://doi.org/10.1016/j.ijbiomac.2021.02.187.
[29] A. Balea, A. Blanco, M. Delgado-Aguilar, M.C. Monte, Q. Tarrés, E. Fuente, et al., Nanocellulose characterization challenges, Bioresources 16 (2021) 4382–4410.
[30] J. Desmaisons, E. Boutonnet, M. Rueff, A. Dufresne, J. Bras, A new quality index for benchmarking of different cellulose nanofibrils, Carbohydr. Polym. 174 (2017) 318–329, https://doi.org/10.1016/j.carbpol.2017.06.032.
[31] C. Moser, M.E. Lindström, G. Henriksson, Toward industrially feasible methods for following the process of manufacturing cellulose nanofibers, Bioresources 10 (2015) 2360–2375.
[32] G. Chinga-Carrasco, Optical methods for the quantification of the fibrillation degree of bleached MFC materials, Micron 48 (2013) 42–48.
[33] Z.J. Jakubek, M. Chen, M. Couillard, T. Leng, L. Liu, S. Zou, et al., Characterization challenges for a cellulose nanocrystal reference material: dispersion and particle size distributions, J. Nanopart. Res. 20 (2018) 1–16.
[34] M. Kaushik, C. Fraschini, G. Chauve, J.L. Putaux, A. Moores, The Transmission Electron Microscopy: Theory and Applications, in: Khan Maaz (Ed.), Transmission electron microscopy for the characterization of cellulose nanocrystals (Chapter 6), IntechOpen, 2015.
[35] F. Gu, W. Wang, Z. Cai, F. Xue, Y. Jin, J.Y. Zhu, Water retention value for characterizing fibrillation degree of cellulosic fibers at micro and nanometer scales, Cellulose 25 (2018) 2861–2871, https://doi.org/10.1007/s10570-018-1765-8.
[36] E.M. Cadena, J. Garcia, T. Vidal, A.L. Torres, Determination of zeta potential and cationic demand in ECF and TCF bleached pulp from eucalyptus and flax. Influence of measuring conditions, Cellulose 16 (2009) 491–500, https://doi.org/10.1007/s10570-009-9275-3.
[37] E. Saarikoski, T. Saarinen, J. Salmela, J. Seppälä, Flocculated flow of microfibrillated cellulose water suspensions: an imaging approach for characterisation of rheological behaviour, Cellulose 19 (2012) 647–659.

[38] M.C. Li, Q. Wu, R.J. Moon, M.A. Hubbe, M.J. Bortner, Rheological aspects of cellulose nanomaterials: governing factors and emerging applications, Adv. Mater. 33 (2021) 2006052.
[39] A.I. Koponen, The effect of consistency on the shear rheology of aqueous suspensions of cellulose micro-and nanofibrils: a review, Cellulose 27 (2020) 1879–1897.
[40] L. Segal, J.J. Creely, A.E. Martin, C.M. Conrad, An empirical method for estimating the degree of crystallinity of native cellulose using the X-ray diffractometer, Text. Res. J. 29 (1959) 786–794, https://doi.org/10.1177/004051755902901003.
[41] J. Patiño-Masó, F. Serra-Parareda, Q. Tarrés, P. Mutjé, F.X.X. Espinach, M. Delgado-Aguilar, TEMPO-oxidized cellulose nanofibers: a potential bio-based superabsorbent for diaper production, Nanomaterials 9 (2019), https://doi.org/10.3390/nano9091271.
[42] M. Delgado-Aguilar, I. González, Q. Tarrés, M.T.À. Pèlach, M. Alcalà, P. Mutjé, The key role of lignin in the production of low-cost lignocellulosic nanofibres for papermaking applications, Ind. Crop. Prod. 86 (2016) 295–300, https://doi.org/10.1016/j.indcrop.2016.04.010.
[43] I. Filipova, F. Serra, Q. Tarrés, P. Mutjé, M. Delgado-Aguilar, Oxidative treatments for cellulose nanofibers production: a comparative study between TEMPO-mediated and ammonium persulfate oxidation, Cellulose 27 (2020) 10671–10688, https://doi.org/10.1007/s10570-020-03089-7.
[44] J.L. Sanchez-Salvador, M.C. Monte, C. Negro, W. Batchelor, G. Garnier, A. Blanco, Simplification of gel point characterization of cellulose nano and microfiber suspensions, Cellulose (2021) 1–12.
[45] C. Campano, A. Balea, Á. Blanco, C. Negro, A reproducible method to characterize the bulk morphology of cellulose nanocrystals and nanofibers by transmission electron microscopy, Cellulose 27 (2020) 4871–4887.
[46] K. Dimic-Misic, A. Puisto, J. Paltakari, M. Alava, T. Maloney, The influence of shear on the dewatering of high consistency nanofibrillated cellulose furnishes, Cellulose 20 (2013) 1853–1864, https://doi.org/10.1007/s10570-013-9964-9.
[47] L. Berglund, M. Noël, Y. Aitomäki, T. Öman, K. Oksman, Production potential of cellulose nanofibers from industrial residues: efficiency and nanofiber characteristics, Ind. Crop. Prod. 92 (2016) 84–92, https://doi.org/10.1016/j.indcrop.2016.08.003.
[48] Z. Wang, S. Winestrand, T. Gillgren, L.J. Jönsson, Chemical and structural factors influencing enzymatic saccharification of wood from aspen, birch and spruce, Biomass Bioenergy 109 (2018) 125–134, https://doi.org/10.1016/j.biombioe.2017.12.020.
[49] J. Leitner, G. Seyfriedsberger, A. Kandelbauer, Modifications in the bulk and the surface of unbleached lignocellulosic fibers induced by a heat treatment without water removal: effects on fibre relaxation of PFI-beaten Kraft fibers, Eur J Wood Wood Prod 71 (2013) 725–738.
[50] Y. Chen, J. Wan, X. Zhang, Y. Ma, Y. Wang, Effect of beating on recycled properties of unbleached eucalyptus cellulose fiber, Carbohydr. Polym. 87 (2012) 730–736.
[51] G.H.D. Tonoli, E.M. Teixeira, A.C. Corrêa, J.M. Marconcini, L.A. Caixeta, M. A. Pereira-da-Silva, et al., Cellulose micro/nanofibres from eucalyptus Kraft pulp: preparation and properties, Carbohydr. Polym. 89 (2012) 80–88.
[52] E. Rojo, M.S. Peresin, W.W. Sampson, I.C. Hoeger, J. Vartiainen, J. Laine, et al., Comprehensive elucidation of the effect of residual lignin on the physical, barrier, mechanical and surface properties of nanocellulose films, Green Chem. 17 (2015) 1853–1866, https://doi.org/10.1039/c4gc02398f.
[53] A. Ferrer, E. Quintana, I. Filpponen, I. Solala, T. Vidal, A. Rodríguez, et al., Effect of residual lignin and heteropolysaccharides in nanofibrillar cellulose and nanopaper from wood fibers, Cellulose (2012), https://doi.org/10.1007/s10570-012-9788-z.
[54] A. Hideno, K. Abe, H. Yano, Preparation using pectinase and characterization of Nanofibers from Orange Peel waste in juice factories, J. Food Sci. 79 (2014), N1218-24, https://doi.org/10.1111/1750-3841.12471.
[55] Q. Tarrés, S. Boufi, P. Mutjé, M. Delgado-Aguilar, Enzymatically hydrolyzed and TEMPO-oxidized cellulose nanofibers for the production of nanopapers: morphological, optical, thermal and mechanical properties, Cellulose 24 (2017) 3943–3954, https://doi.org/10.1007/s10570-017-1394-7.
[56] Q. Tarrés, E. Espinosa, J. Domínguez-Robles, A. Rodríguez, P. Mutjé, M. Delgado-Aguilar, The suitability of banana leaf residue as raw material for the production of high lignin content micro/nano fibers: from residue to value-added products, Ind. Crop. Prod. 99 (2017) 27–33, https://doi.org/10.1016/j.indcrop.2017.01.021.
[57] Q. Tarrés, N.V. Ehman, M.E. Vallejos, M.C. Area, M. Delgado-Aguilar, P. Mutjé, Lignocellulosic nanofibers from triticale straw: the influence of hemicelluloses and lignin in their production and properties, Carbohydr. Polym. 163 (2017) 20–27.
[58] Q. Cheng, S. Wang, T.G. Rials, S.H. Lee, Physical and mechanical properties of polyvinyl alcohol and polypropylene composite materials reinforced with fibril aggregates isolated from regenerated cellulose fibers, Cellulose 14 (2007) 593–602.
[59] T. Yuan, J. Zeng, B. Wang, Z. Cheng, K. Chen, Lignin containing cellulose nanofibers (LCNFs): lignin content-morphology-rheology relationships, Carbohydr. Polym. 254 (2021), 117441.
[60] H.Q. Lê, K. Dimic-Misic, L.S. Johansson, T. Maloney, H. Sixta, Effect of lignin on the morphology and rheological properties of nanofibrillated cellulose produced from ?-valerolactone/water fractionation process, Cellulose 25 (2018) 179–194.
[61] Y. Jiang, X. Liu, Q. Yang, X. Song, C. Qin, S. Wang, et al., Effects of residual lignin on composition, structure and properties of mechanically defibrillated cellulose fibrils and films, Cellulose 26 (2019) 1577–1593.
[62] M. Pääkkö, J. Vapaavuori, R. Silvennoinen, H. Kosonen, M. Ankerfors, T. Lindström, et al., Long and entangled native cellulose I nanofibers allow flexible aerogels and hierarchically porous templates for functionalities, Soft Matter 4 (2008) 2492–2499.
[63] M.L. Hassan, A.P. Mathew, E.A. Hassan, N.A. El-Wakil, K. Oksman, Nanofibers from bagasse and rice straw: process optimization and properties, Wood Sci. Technol. 46 (2012) 193–205.
[64] J. Zeng, F. Hu, Z. Cheng, B. Wang, K. Chen, Isolation and rheological characterization of cellulose nanofibrils (CNFs) produced by microfluidic homogenization, ball-milling, grinding and refining, Cellulose (2021) 1–20.
[65] R. Tanaka, T. Saito, D. Ishii, A. Isogai, Determination of nanocellulose fibril length by shear viscosity measurement, Cellulose 21 (2014) 1581–1589.
[66] J.L. Sanchez-Salvador, M.C. Monte, W. Batchelor, G. Garnier, C. Negro, A. Blanco, Characterizing highly fibrillated nanocellulose by modifying the gel point methodology, Carbohydr. Polym. 227 (2020), 115340.
[67] T. Pettersson, J. Hellwig, P. Gustafsson, S. Stenström, Measurement of the flexibility of wet cellulose fibres using atomic force microscopy, Cellulose 24 (2017) 4139–4149.
[68] A. Lourenço, H. Pereira, Compositional variability of lignin in biomass, Lignin—Trends Appl. 10 (2018).
[69] T. Moberg, K. Sahlin, K. Yao, S. Geng, G. Westman, Q. Zhou, et al., Rheological properties of nanocellulose suspensions: effects of fibril/particle dimensions and surface characteristics, Cellulose 24 (2017) 2499–2510.
[70] R. Tanaka, T. Saito, H. Hondo, A. Isogai, Influence of flexibility and dimensions of nanocelluloses on the flow properties of their aqueous dispersions, Biomacromolecules 16 (2015) 2127–2131.
[71] A. Karppinen, A.H. Vesterinen, T. Saarinen, P. Pietikäinen, J. Seppälä, Effect of cationic polymethacrylates on the rheology and flocculation of microfibrillated cellulose, Cellulose 18 (2011) 1381–1390.
[72] A.E. Horvath, T. Lindström, The influence of colloidal interactions on fiber network strength, J. Colloid Interface Sci. 309 (2007) 511–517.
[73] X. Xiong, S. Guo, Z. Xu, P. Sheng, P. Tong, Development of an atomic-force-microscope-based hanging-fiber rheometer for interfacial microrheology, Phys. Rev. E 80 (2009), 061604.